

Supplementary Information for:

Fabricating an intelligent cell-like nano-prodrug *via* the hierarchical self-assembly based on DNA skeleton for lung metastasis of breast cancer therapy†

Yunyan Li,^{‡a} Tong Yan,^{‡a} Wenya Chang,^b Chongjiang Cao^{*,c} and Dawei Deng^{*,a,b}

^aDepartment of Biomedical Engineering, ^bDepartment of Pharmaceutical Engineering, and ^c National R&D Center for Chinese Herbal Medicine Processing, School of Engineering, China Pharmaceutical University, Nanjing 211198, P. R. China

[‡] These authors contributed equally to this work.

* Corresponding authors.

Email: dengdawei@cpu.edu.cn (D. D), chongjiangcao@cpu.edu.cn (C. C.)

Table S1. DNA sequences used in this work.

Oligonucleotide	Sequences (from 5' to 3')
T_{0a}	CTG TCA TCG GTC AC ACA TTC CTA AGT CTG AAA CAT TAC AGC TTG CTA CAC GAG AAG AGC CGC CAT AGT A
T_{0b}	CTG TCA TCG GTC AC TAT CAC CAG GCA GTT GAC AGT GTA GCA AGC TGT AAT AGA TGC GAG GGT CCA ATA C
T_{0c}	CTG TCA TCG GTC AC TCA ACT GCC TGG TGA TAA AAC GAC ACT ACG TGG GAA TCT ACT ATG GCG GCT CTT C
T_{0d}	CTG TCA TCG GTC AC TTC AGA CTT AGG AAT GTG CTT CCC ACG TAG TGT CGT TTG TAT TGG ACC CTC GCA
T_{1a}	GAA GCC ACT CTG AT ACA TTC CTA AGT CTG AAA CAT TAC AGC TTG CTA CAC GAG AAG AGC CGC CAT AGT A
T_{1b}	GTG ACC GAT GAC AG TAT CAC CAG GCA GTT GAC AGT GTA GCA AGC TGT AAT AGA TGC GAG GGT CCA ATA C
T_{1c}	GAA GCC ACT CTG AT TCA ACT GCC TGG TGA TAA AAC GAC ACT ACG TGG GAA TCT ACT ATG GCG GCT CTT C
T_{1d}	GAA GCC ACT CTG AT TTC AGA CTT AGG AAT GTG CTT CCC ACG TAG TGT CGT TTG TAT TGG ACC CTC GCA T
T_{2a}	GAC CGA TGG ATG AG ACA TTC CTA AGT CTG AAA CAT TAC AGC TTG CTA CAC GAG AAG AGC CGC CAT AGT A
T_{2b}	ATC AGA GTG GCT TC TAT CAC CAG GCA GTT GAC AGT GTA GCA AGC TGT AAT AGA TGC GAG GGT CCA ATA C
T_{2c}	GAC CGA TGG ATG AG TCA ACT GCC TGG TGA TAA AAC GAC ACT ACG TGG GAA TCT ACT ATG GCG GCT CTT C
T_{2d}	GAC CGA TGG ATG AG TTC AGA CTT AGG AAT GTG CTT CCC ACG TAG TGT CGT TTG TAT TGG ACC CTC GCA T
SH-DNA	CTCATCCATCGGTC-C6-SH

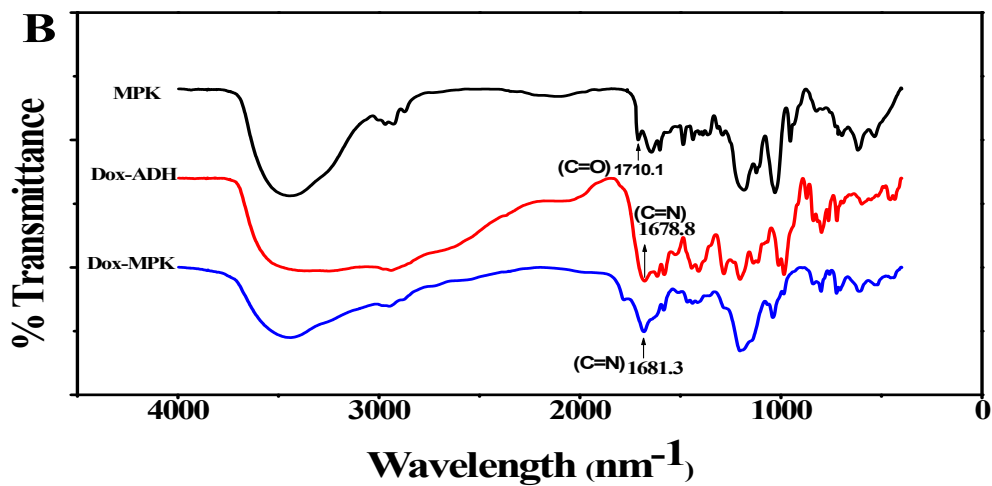
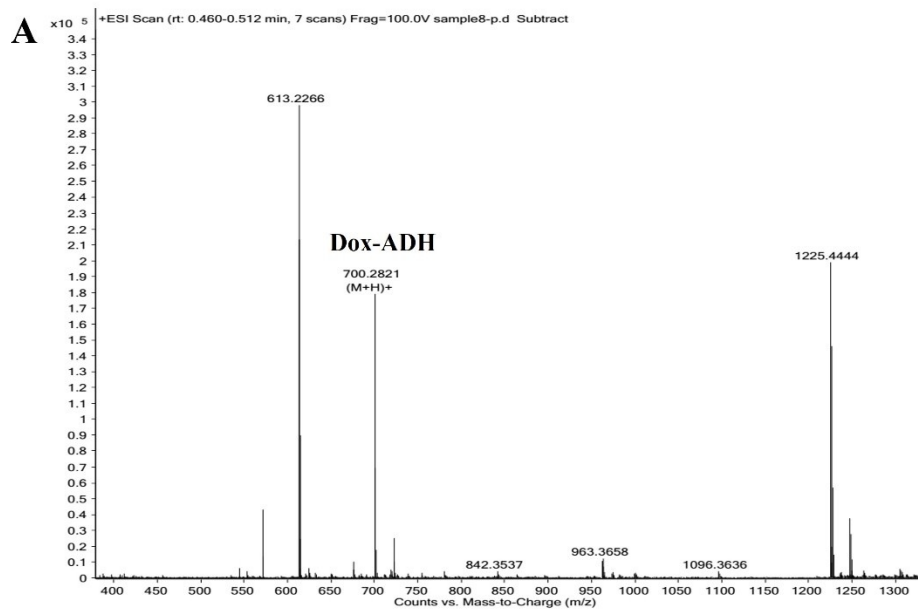


Figure S1. (A) The mass spectrum of Dox-ADH ($m/z = 700$ [$M+ +1$, $\text{C}_{33}\text{H}_{41}\text{N}_5\text{O}_{12}$]). (B) FT-IR spectra of MPK, Dox-ADH, and Dox-MPK.

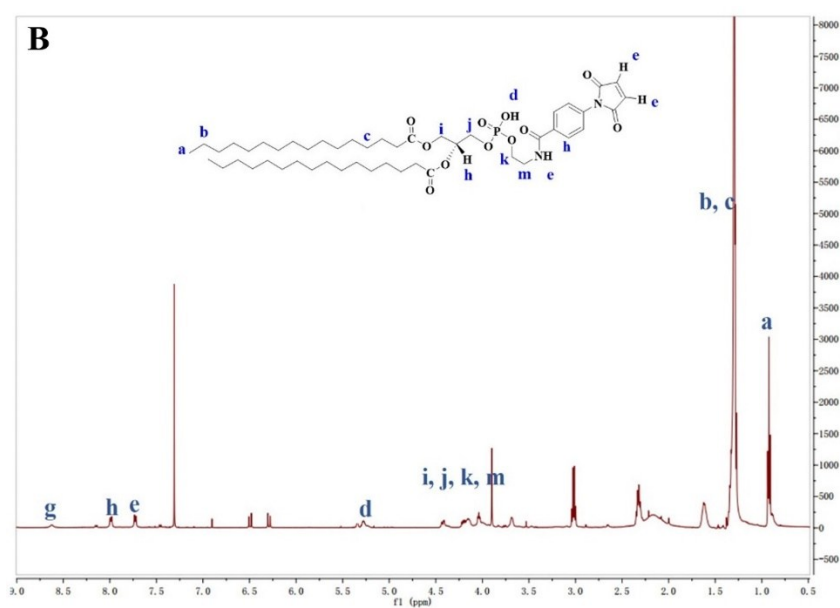
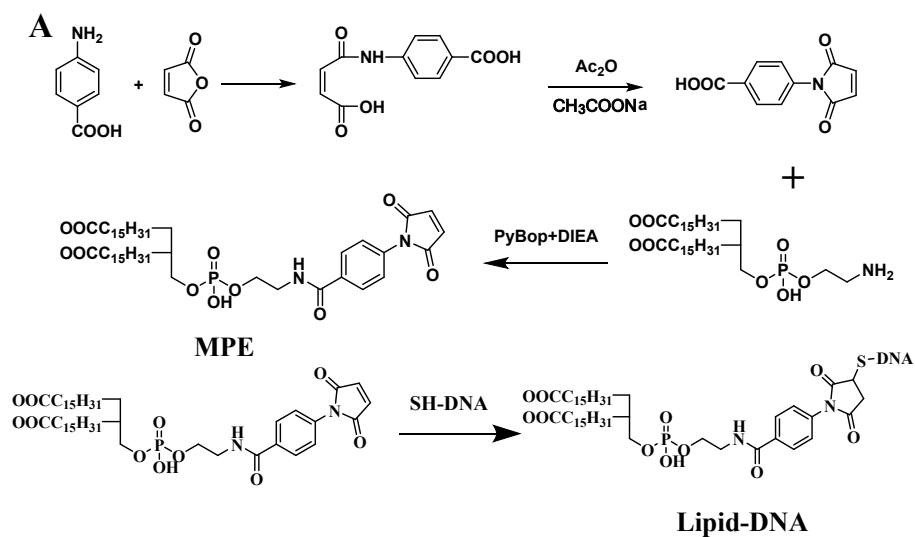


Figure S2. (A) The synthesis procedure of Lipid-DNA. (B) The ^1H -NMR spectra of MPE.

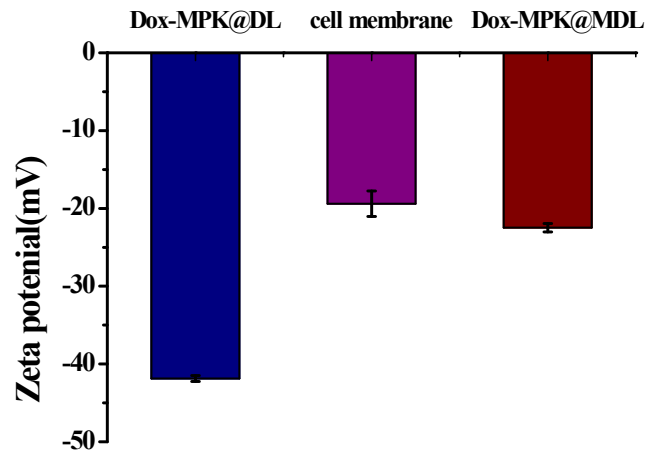


Figure S3. Surface charge of Dox-MPK@DL, macrophage membrane, and Dox-MPK@MDL, n=3.

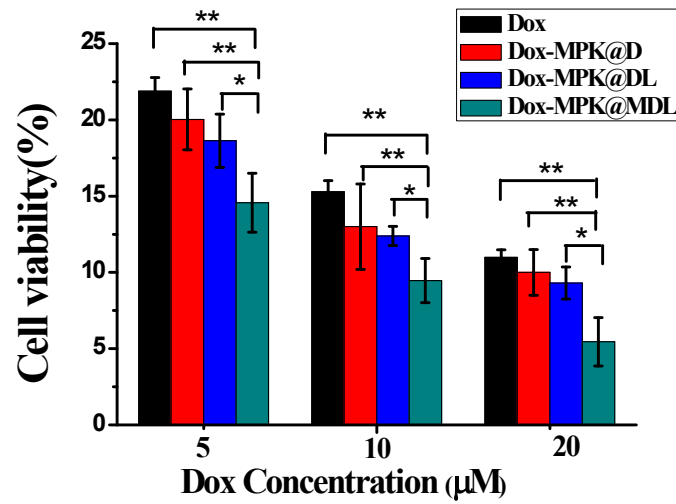


Figure S4. Cytotoxicity of each group at different concentrations of Dox, n=6, *p < 0.05, **p < 0.01

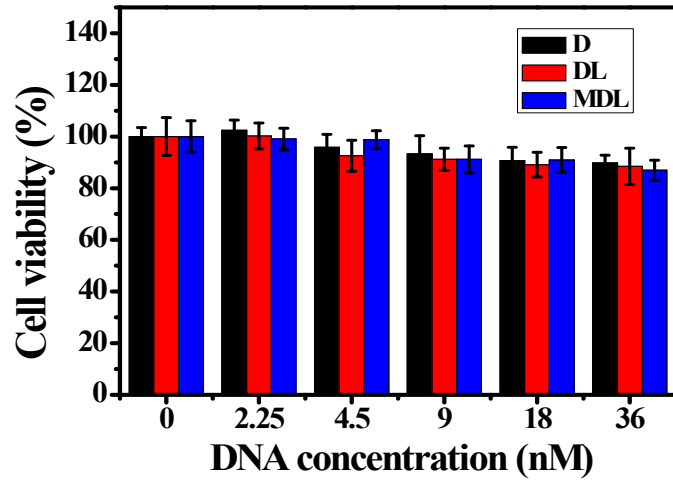


Figure S5. Cytotoxicity of blank D, DL and MDL without Dox in metastatic 4T1 cancer cells, n=6.

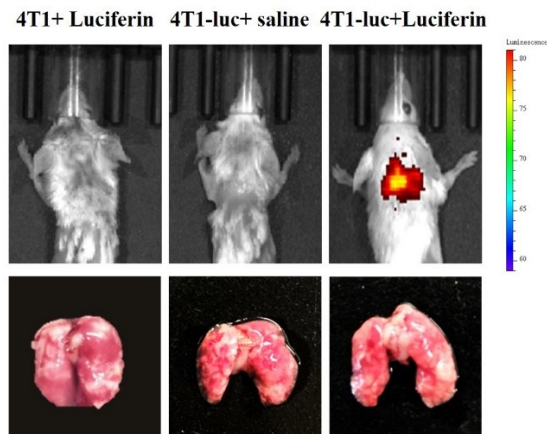


Figure S6. In vivo bioluminescence imaging of lung metastasis and photograph of lung lung tissues on the fourteenth day.

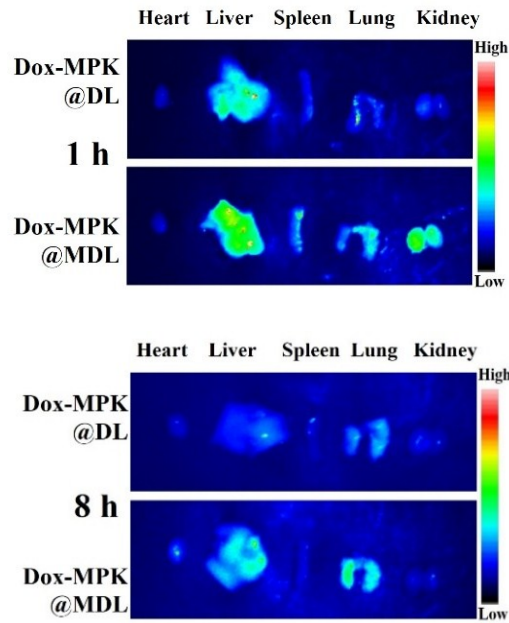


Figure S7. Corresponding ex vivo imaging of major organs at 1 h and 8 h post-injection.

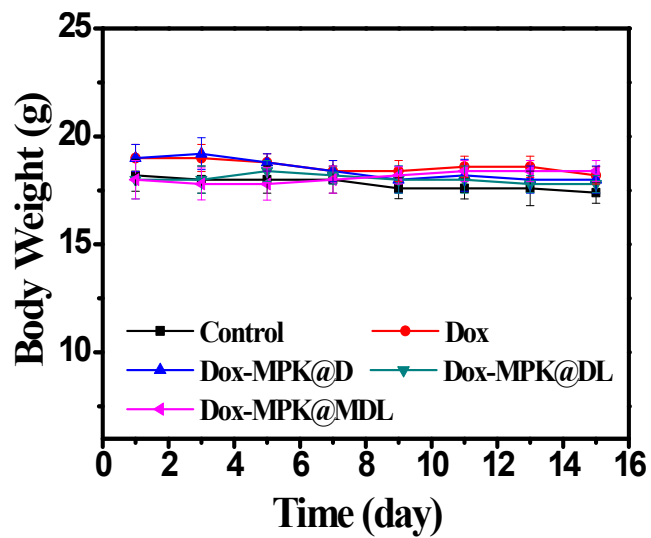


Figure S8. Body weight of each group of mice during the treatment period, n=5.

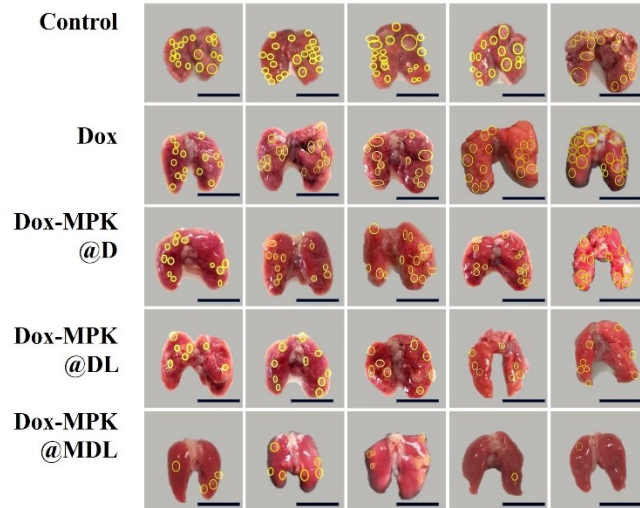


Figure S9. Typical photographs of lung tissues from each group, scale bar = 1 cm.

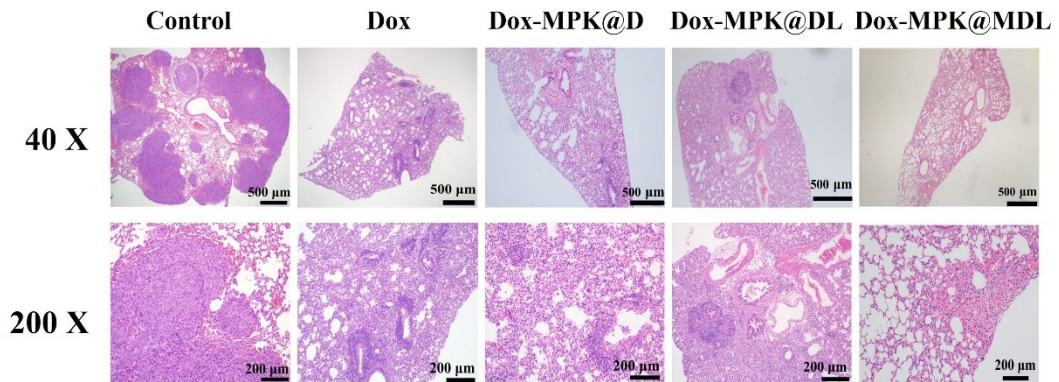


Figure S10. Histopathology sections of metastatic lesions in lung tissues from each group.